Extended Block-Lifting-based Lapped Transforms

Taizo Suzuki, *Member, IEEE* and Hiroyuki Kudo, *Member, IEEE*

***Abstract*—We extend an original lapped transform (LT) and use block-lifting factorization to get an extended block-lifting-based LT (XBL-LT). The block-lifting structure maps integer input signals to integer output signals and results in a reversible transform that reduces rounding errors by merging many rounding operations. Although other such block-lifting-based LTs (BL-LTs) have been proposed, they are forcibly constrained by the use of discrete cosine transform (DCT) matrices. In contrast, XBL-LT is DCT-unconstrained and hence also embodies the DCT-constrained form. Furthermore, it has fewer rounding operations by merging the scaling factor with block-lifting coefficients. The both DCT-constrained and unconstrained XBL-LTs perform well at lossy-to-lossless image coding which has scalability from lossless data to lossy data.**

***Index Terms*—Block-lifting structure, lapped transform (LT), lossy-to-lossless image coding**

I. Introduction

LAPPED transforms (LTs) [1] are popular subband transforms that can be used as substitutes for the discrete cosine transform (DCT) [2] used in image/video compression (image coding). Although almost all of the JPEG and H.26x series [3–5], image coding standards, use DCTs for their good energy compaction, DCT-based image codings generate unpleasant artifacts, i.e., blocking artifacts, at low bit rates due to their ignoring the continuity of the blocks. LT-based image coding solves that problem by using a processing that works over the blocks.

The lifting structure [6] is a very important technology to achieve a lossless mode in subband transform-based image coding. It maps integer input signals to integer output signals; i.e., it is an integer-to-integer transform. The 4×8 lifting-based LT (L-LT) [7] in JPEG XR [8], the newest image coding standard, is a time-domain LT (TDLT) [9] with simple scaling factors and lifting structures. In spite of its simple structure, it performs well at lossy-to-lossless image coding, which has scalability from lossless to lossy data. The block-lifting structure [10] is a class of lifting structures and results in a reversible transform that reduces rounding errors by merging many rounding operations. Inspired by the L-LT in JPEG XR, we have proposed block-lifting-based LTs (BL-LTs) [11], [12] that perform well with larger block size than those of the L-LT in JPEG XR. However, they are forcibly DCT-constrained and degrade coding performance at high bit rates.

Here, we extend an original LT and use block-lifting factorization to get an extended BL-LT (XBL-LT). The XBL-LT is DCT-unconstrained, unlike the BL-LTs presented in [11], [12], and hence also embodies the DCT-constrained form. Furthermore, more rounding operations than the methods described in our previous studies are removed by merging the scaling factor with block-lifting coefficients. As a result, the both DCT-constrained and unconstrained XBL-LTs perform well at lossy-to-lossless image coding.

Notation: The italic letter M ($M = 2^n$, $n \in \mathbb{N}$) denotes the block size. Boldface letters $\mathbf{I}_m$, $\mathbf{J}_m$, $\mathbf{0}$, and $\mathbf{D}_m$ denote an $m \times m$ identity matrix, an $m \times m$ reversal matrix, a null matrix, and an $m \times m$ diagonal matrix with alternating ± 1 entries (i.e., $\mathrm{diag}\{1, -1, 1, -1, \cdots\}$), respectively. The superscripts T and -1 respectively mean the transpose and inverse of a matrix.

T. Suzuki and H. Kudo are with the Faculty of Engineering, Information and Systems, University of Tsukuba, Tsukuba, Ibaraki, 305-8573 Japan (e-mail: {taizo, kudo}@cs.tsukuba.ac.jp).

II. Review and Definition

A. Lapped Transform (LT)

In accordance with [11], [12], let $\mathbf{E}(z)$ be a polyphase matrix of an $M \times 2M$ LT with a scaling factor s derived from the L-LT in JPEG XR [7]:

$$\mathbf{E}(z) = \mathbf{P} \begin{bmatrix} \mathbf{I}_N & \mathbf{0} \\ \mathbf{0} & \boldsymbol{\mathcal{S}}_N^{IV} \boldsymbol{\mathcal{C}}_N^{III} \end{bmatrix} \boldsymbol{\Gamma}(z) \begin{bmatrix} \boldsymbol{\mathcal{C}}_N^{II} & \mathbf{0} \\ \mathbf{0} & \boldsymbol{\mathcal{C}}_N^{IV} \mathbf{J}_N \end{bmatrix} \mathbf{S} \widetilde{\mathbf{W}} \mathbf{J}_M, \tag{1}$$

where

$$\begin{aligned} \boldsymbol{\Gamma}(z) &= \mathbf{W} \boldsymbol{\Lambda}(z) \mathbf{W}, \ \boldsymbol{\Lambda}(z) = \mathrm{diag}\{\mathbf{I}_N, z^{-1}\mathbf{I}_N\} \\ \mathbf{W} &= \frac{1}{\sqrt{2}} \begin{bmatrix} \mathbf{I}_N & \mathbf{I}_N \\ \mathbf{I}_N & -\mathbf{I}_N \end{bmatrix}, \ \widetilde{\mathbf{W}} = \frac{1}{\sqrt{2}} \begin{bmatrix} \mathbf{I}_N & \mathbf{J}_N \\ \mathbf{J}_N & -\mathbf{I}_N \end{bmatrix} \\ \mathbf{S} &= \mathrm{diag}\{s\mathbf{I}_N, s^{-1}\mathbf{I}_N\}. \end{aligned}$$

$\boldsymbol{\mathcal{C}}_M^X$ and $\boldsymbol{\mathcal{S}}_M^X$ are type-X DCT (DCT-X) and type-X discrete sine transform (DST-X) matrices, and the (i, j)-elements of $\boldsymbol{\mathcal{C}}_M^{II}$ and $\boldsymbol{\mathcal{C}}_M^{IV}$ are

$$\begin{aligned} \left[\boldsymbol{\mathcal{C}}_M^{II}\right]_{i,j} &= \sqrt{\frac{2}{M}} c_i \cos\left(\frac{i\,(j+1/2)\,\pi}{M}\right) \\ \left[\boldsymbol{\mathcal{C}}_M^{IV}\right]_{i,j} &= \sqrt{\frac{2}{M}} \cos\left(\frac{(i+1/2)\,(j+1/2)\,\pi}{M}\right), \end{aligned}$$

where $c_k = 1/\sqrt{2}$ ($k = 0$) or 1 ($k \neq 0$), respectively. The following relationships between matrices can be established:

$$\boldsymbol{\mathcal{C}}_M^{III} = \left(\boldsymbol{\mathcal{C}}_M^{II}\right)^{-1} = \left(\boldsymbol{\mathcal{C}}_M^{II}\right)^T, \ \boldsymbol{\mathcal{S}}_M^{IV} = \mathbf{D}_M \boldsymbol{\mathcal{C}}_M^{IV} \mathbf{J}_M. \tag{2}$$

Here, $\mathbf{P}$ is an $M \times M$ permutation matrix. The optimal scaling s in $\mathbf{S}$ is empirically determined, e.g., $s = 0.8981$ if $M = 8$ and 0.9360 if $M = 16$. Since the LT in Eq. (1) with $s = 1$ is completely equivalent to a lapped orthogonal transform (LOT), we will use the LT in Eq. (1) as a representative expression of LT.

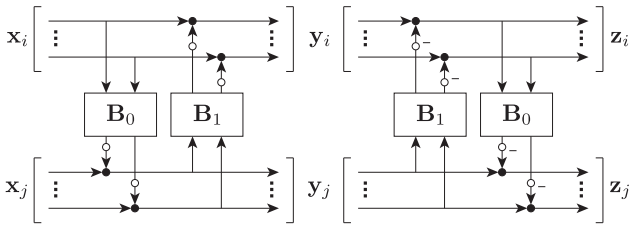

Fig. 1. Block-lifting structure (black and white circles mean adders and rounding operations, respectively).

B. Block-Lifting Structure

The block-lifting structure [10] (Fig. 1) is a class of lifting structures. The structure can be expressed as follows:

$$\mathbf{y}_j = \mathbf{x}_j + \text{round}(\mathbf{B}_0\mathbf{x}_i), \qquad \mathbf{y}_i = \mathbf{x}_i + \text{round}(\mathbf{B}_1\mathbf{y}_j)$$
$$\mathbf{z}_i = \mathbf{y}_i - \text{round}(\mathbf{B}_1\mathbf{y}_j) = \mathbf{x}_i, \mathbf{z}_j = \mathbf{y}_j - \text{round}(\mathbf{B}_0\mathbf{z}_i) = \mathbf{x}_j,$$

where $\mathbf{x}_\times$, $\mathbf{y}_\times$, and $\mathbf{z}_\times$ are $N \times 1$ input/output vector signals, round$(\cdot)$ is a rounding operation, and the block-lifting coefficients $\mathbf{B}_0$ and $\mathbf{B}_1$ are $N \times N$ arbitrary matrices. In this case, the matrices and their inverses are expressed as lower and upper block-lifting matrices as follows:

$$\mathfrak{L}\left[\mathbf{B}_0\right] \triangleq \begin{bmatrix} \mathbf{I}_N & \mathbf{0} \\ \mathbf{B}_0 & \mathbf{I}_N \end{bmatrix}, \ \mathfrak{L}\left[\mathbf{B}_0\right]^{-1} = \mathfrak{L}\left[-\mathbf{B}_0\right]$$
$$\mathfrak{U}\left[\mathbf{B}_1\right] \triangleq \begin{bmatrix} \mathbf{I}_N & \mathbf{B}_1 \\ \mathbf{0} & \mathbf{I}_N \end{bmatrix}, \ \mathfrak{U}\left[\mathbf{B}_1\right]^{-1} = \mathfrak{U}\left[-\mathbf{B}_1\right].$$

Rounding errors generated by the rounding operation in each lifting step degrade coding performance. The block-lifting structure reduces such rounding errors by merging many rounding operations. A special class of block-lifting structure is expressed as [13]

$$\begin{bmatrix} \mathbf{M} & \mathbf{0} \\ \mathbf{0} & \mathbf{M}^{-1} \end{bmatrix} = \mathfrak{L}\left[\mathbf{M}^{-1}\right] \mathfrak{U}\left[-\mathbf{M}\right] \mathfrak{L}\left[\mathbf{M}^{-1}\right] \widetilde{\mathbf{J}}_M \quad (3)$$
$$= \widehat{\mathbf{J}}_M \mathfrak{L}\left[-\mathbf{M}\right] \mathfrak{U}\left[\mathbf{M}^{-1}\right] \mathfrak{L}\left[-\mathbf{M}\right], \quad (4)$$

where

$$\widetilde{\mathbf{J}}_M = \begin{bmatrix} \mathbf{0} & \mathbf{I}_N \\ -\mathbf{I}_N & \mathbf{0} \end{bmatrix}, \quad \widehat{\mathbf{J}}_M = \begin{bmatrix} \mathbf{0} & -\mathbf{I}_N \\ \mathbf{I}_N & \mathbf{0} \end{bmatrix},$$

and $\mathbf{M}$ is an $N \times N$ arbitrary nonsingular matrix.

III. Extended Block-Lifting-based Lapped Transform (XBL-LT)

Theorem: We can extend the DCT-constrained LT in Eq. (1) to a DCT-unconstrained LT as follows:

$$\mathbf{E}(z) = \mathbf{P} \begin{bmatrix} \mathbf{I}_N & \mathbf{0} \\ \mathbf{0} & \mathbf{D}_N\widetilde{\boldsymbol{\mathcal{V}}}^{-1}\mathbf{J}_N\widetilde{\boldsymbol{\mathcal{U}}}^{-1} \end{bmatrix} \boldsymbol{\Gamma}(z) \begin{bmatrix} \widetilde{\boldsymbol{\mathcal{U}}} & \mathbf{0} \\ \mathbf{0} & \widetilde{\boldsymbol{\mathcal{V}}}\mathbf{J}_N \end{bmatrix} \mathbf{S}\widetilde{\mathbf{W}}\mathbf{J}_M,$$

where $\widetilde{\boldsymbol{\mathcal{U}}}$ and $\widetilde{\boldsymbol{\mathcal{V}}}$ are $N \times N$ arbitrary nonsingular matrices. This equation can be simplified as

$$\mathbf{E}(z) = \mathbf{P} \begin{bmatrix} \mathbf{I}_N & \mathbf{0} \\ \mathbf{0} & \boldsymbol{\mathcal{V}}^{-1}\mathbf{J}_N\boldsymbol{\mathcal{U}}^{-1} \end{bmatrix} \boldsymbol{\Gamma}(z) \begin{bmatrix} \boldsymbol{\mathcal{U}} & \mathbf{0} \\ \mathbf{0} & \boldsymbol{\mathcal{V}}\mathbf{J}_N \end{bmatrix} \widehat{\mathbf{W}}\mathbf{J}_M, \quad (5)$$

where

$$\boldsymbol{\mathcal{U}} = \sqrt{2}s\,\widetilde{\boldsymbol{\mathcal{U}}}, \ \boldsymbol{\mathcal{V}} = \frac{1}{\sqrt{2}s}\widetilde{\boldsymbol{\mathcal{V}}}, \ \widehat{\mathbf{W}} = \begin{bmatrix} \frac{1}{2}\mathbf{I}_N & \frac{1}{2}\mathbf{J}_N \\ \mathbf{J}_N & -\mathbf{I}_N \end{bmatrix},$$

by using Eq. (2) and skipping the sign inversion matrix $\mathbf{D}_N$. The scaling matrix $\mathbf{S}$ is being embedded in $\boldsymbol{\mathcal{U}}$ and $\boldsymbol{\mathcal{V}}$. When $\widetilde{\boldsymbol{\mathcal{U}}} = \boldsymbol{\mathcal{C}}_N^{II}$ and $\widetilde{\boldsymbol{\mathcal{V}}} = \boldsymbol{\mathcal{C}}_N^{IV}$, the LT in Eq. (5) is completely equivalent to the LT in Eq. (1) except that the signs are different. Then, we factorize the LT in Eq. (5) into block-lifting structures as

$$\mathbf{E}(z) = \mathbf{P}\mathfrak{L}\left[\boldsymbol{\mathcal{B}}_4\right]\mathfrak{U}\left[\boldsymbol{\mathcal{B}}_3\right]\boldsymbol{\Lambda}(z)\mathfrak{U}\left[\boldsymbol{\mathcal{B}}_3\right]\mathfrak{L}\left[\boldsymbol{\mathcal{B}}_2\right]\mathfrak{U}\left[\boldsymbol{\mathcal{B}}_1\right]\mathfrak{L}\left[\boldsymbol{\mathcal{B}}_0\right]$$
$$\cdot\,\mathfrak{U}\left[-\frac{1}{2}\mathbf{J}_N\right]\mathfrak{L}\left[\mathbf{J}_N\right]\widetilde{\mathbf{J}}_M, \quad (6)$$

wherein each matrix is defined as

$$\boldsymbol{\mathcal{B}}_0 = -\boldsymbol{\mathcal{V}}^{-1}, \ \boldsymbol{\mathcal{B}}_1 = \boldsymbol{\mathcal{V}}, \ \boldsymbol{\mathcal{B}}_2 = \boldsymbol{\mathcal{B}}_0 + \boldsymbol{\mathcal{B}}_4$$
$$\boldsymbol{\mathcal{B}}_3 = -\frac{1}{2}\boldsymbol{\mathcal{U}}\mathbf{J}_N\boldsymbol{\mathcal{V}}, \ \boldsymbol{\mathcal{B}}_4 = \boldsymbol{\mathcal{V}}^{-1}\mathbf{J}_N\boldsymbol{\mathcal{U}}^{-1}.$$

Actually, the block-lifting matrices $\mathfrak{U}\left[\boldsymbol{\mathcal{B}}_3\right]$ on both sides of the delay matrix $\boldsymbol{\Lambda}(z)$ are collectively implemented, as shown in Fig. 2.

Proof: We can perform an easy matrix manipulation as follows:

$$\begin{bmatrix} \mathbf{M}_0 & \mathbf{0} \\ \mathbf{0} & \mathbf{M}_1 \end{bmatrix} \begin{bmatrix} \mathbf{I}_N & \mathbf{N}_0 \\ \mathbf{N}_1 & \mathbf{I}_N \end{bmatrix}$$
$$= \begin{bmatrix} \mathbf{I}_N & \mathbf{M}_0\mathbf{N}_0\mathbf{M}_1^{-1} \\ \mathbf{M}_1\mathbf{N}_1\mathbf{M}_0^{-1} & \mathbf{I}_N \end{bmatrix} \begin{bmatrix} \mathbf{M}_0 & \mathbf{0} \\ \mathbf{0} & \mathbf{M}_1 \end{bmatrix},$$

where $\mathbf{M}_\times$ and $\mathbf{N}_\times$ are an $N \times N$ arbitrary nonsingular matrix and $N \times N$ arbitrary matrix, respectively. First, $\boldsymbol{\Gamma}(z)$ in Eq. (5) can easily be represented by

$$\boldsymbol{\Gamma}(z) = \mathfrak{L}\left[\mathbf{I}_N\right]\mathfrak{U}\left[-\frac{1}{2}\mathbf{I}_N\right]\boldsymbol{\Lambda}(z)\mathfrak{U}\left[\frac{1}{2}\mathbf{I}_N\right]\mathfrak{L}\left[-\mathbf{I}_N\right].$$

Next, $\boldsymbol{\mathcal{U}}^{-1}$ in Eq. (5) is moved to the right side of $\boldsymbol{\Gamma}(z)$ and simplified as

$$\boldsymbol{\Psi}(z) \triangleq \begin{bmatrix} \mathbf{I}_N & \mathbf{0} \\ \mathbf{0} & \boldsymbol{\mathcal{U}}^{-1} \end{bmatrix} \boldsymbol{\Gamma}(z) \begin{bmatrix} \boldsymbol{\mathcal{U}} & \mathbf{0} \\ \mathbf{0} & \mathbf{I}_N \end{bmatrix}$$
$$= \mathfrak{L}\left[\boldsymbol{\mathcal{U}}^{-1}\right]\mathfrak{U}\left[-\frac{1}{2}\boldsymbol{\mathcal{U}}\right]\boldsymbol{\Lambda}(z)\mathfrak{U}\left[\frac{1}{2}\boldsymbol{\mathcal{U}}\right]\mathfrak{L}\left[-\boldsymbol{\mathcal{U}}^{-1}\right]\begin{bmatrix} \boldsymbol{\mathcal{U}} & \mathbf{0} \\ \mathbf{0} & \boldsymbol{\mathcal{U}}^{-1} \end{bmatrix}$$
$$= \mathfrak{L}\left[\boldsymbol{\mathcal{U}}^{-1}\right]\mathfrak{U}\left[-\frac{1}{2}\boldsymbol{\mathcal{U}}\right]\boldsymbol{\Lambda}(z)\mathfrak{U}\left[-\frac{1}{2}\boldsymbol{\mathcal{U}}\right]\mathfrak{L}\left[\boldsymbol{\mathcal{U}}^{-1}\right]\widetilde{\mathbf{J}}_M,$$

because the block diagonal matrix $\text{diag}\{\boldsymbol{\mathcal{U}}, \boldsymbol{\mathcal{U}}^{-1}\}$ in $\boldsymbol{\Psi}(z)$ can be factorized into block-lifting structures as in Eq. (3). Then, $\boldsymbol{\mathcal{V}}^{-1}\mathbf{J}_N$ in Eq. (5) is moved to the right side of $\boldsymbol{\Psi}(z)$ and

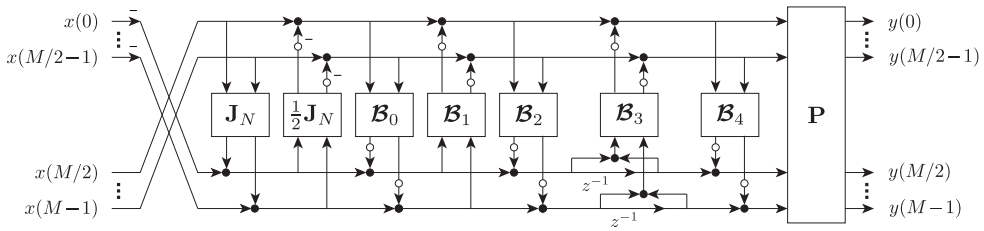

Fig. 2. XBL-LT (black and white circles mean adders and rounding operations, respectively).

TABLE I
CODING GAINS OF XBL-LTS.

Block Size	DCT-Constrained	DCT-Unconstrained
8	9.4475	**9.4538**
16	9.8455	**9.8621**

TABLE II
NUMBERS OF ROUNDING OPERATIONS OF BL-LTS.

Block Size	BL-LT [11]	BL-LT [12]	XBL-LT
8	48	28	**24**
16	96	56	**48**
M	$6M$	$7M/2$	$\mathbf{3}\boldsymbol{M}$

simplified as

$$\begin{aligned}\boldsymbol{\Omega}(z) &\triangleq \begin{bmatrix}\mathbf{I}_N & \mathbf{0}\\ \mathbf{0} & \boldsymbol{\mathcal{V}}^{-1}\mathbf{J}_N\end{bmatrix}\boldsymbol{\Psi}(z)\begin{bmatrix}\mathbf{I}_N & \mathbf{0}\\ \mathbf{0} & \boldsymbol{\mathcal{V}}\mathbf{J}_N\end{bmatrix}\\ &= \mathfrak{L}\left[\boldsymbol{\mathcal{W}}^{-1}\right]\mathfrak{U}\left[-\frac{1}{2}\boldsymbol{\mathcal{W}}\right]\boldsymbol{\Lambda}(z)\mathfrak{U}\left[-\frac{1}{2}\boldsymbol{\mathcal{W}}\right]\\ &\quad\cdot\mathfrak{L}\left[\boldsymbol{\mathcal{W}}^{-1}\right]\widetilde{\mathbf{J}}_M\begin{bmatrix}\boldsymbol{\mathcal{V}}^{-1}\mathbf{J}_N & \mathbf{0}\\ \mathbf{0} & \boldsymbol{\mathcal{V}}\mathbf{J}_N\end{bmatrix}\\ &= \mathfrak{L}\left[\boldsymbol{\mathcal{W}}^{-1}\right]\mathfrak{U}\left[-\frac{1}{2}\boldsymbol{\mathcal{W}}\right]\boldsymbol{\Lambda}(z)\mathfrak{U}\left[-\frac{1}{2}\boldsymbol{\mathcal{W}}\right]\\ &\quad\cdot\mathfrak{L}\left[\boldsymbol{\mathcal{W}}^{-1}-\boldsymbol{\mathcal{V}}^{-1}\right]\mathfrak{U}[\boldsymbol{\mathcal{V}}]\,\mathfrak{L}\left[-\boldsymbol{\mathcal{V}}^{-1}\right]\begin{bmatrix}\mathbf{J}_N & \mathbf{0}\\ \mathbf{0} & \mathbf{J}_N\end{bmatrix},\end{aligned}$$

where $\boldsymbol{\mathcal{W}} = \boldsymbol{\mathcal{U}}\mathbf{J}_N\boldsymbol{\mathcal{V}}$, because the block diagonal matrix $\mathrm{diag}\{\boldsymbol{\mathcal{V}}^{-1},\boldsymbol{\mathcal{V}}\}$ in $\boldsymbol{\Omega}(z)$ can also be factorized into block-lifting structures as in Eq. (4). Finally, the residual part $\widehat{\mathbf{W}}\mathbf{J}_M$ in Eq. (5) and $\mathrm{diag}\{\mathbf{J}_N,\mathbf{J}_N\}$ in $\boldsymbol{\Omega}(z)$ are collectively factorized as

$$\begin{bmatrix}\mathbf{J}_N & \mathbf{0}\\ \mathbf{0} & \mathbf{J}_N\end{bmatrix}\widehat{\mathbf{W}}\mathbf{J}_M = \mathfrak{U}\left[-\frac{1}{2}\mathbf{J}_N\right]\mathfrak{L}\left[\mathbf{J}_N\right]\widetilde{\mathbf{J}}_M.$$

□

IV. EXPERIMENTAL RESULTS

A. Coding Gain, Frequency Response, and Number of Rounding Operations

We designed 8×16 and 16×32 XBL-LTs by optimizing the coding gain (CG) [14]

$$\text{CG [dB]} = 10\log_{10}\frac{\sigma_x^2}{\prod_{k=0}^{M-1}\sigma_{x_k}^2\parallel f_k\parallel^2},$$

where σ_x^2 is the variance of the input signal, $\sigma_{x_k}^2$ is the variance of the k-th subbands and $\parallel f_k \parallel^2$ is the norm of the k-th synthesis filter. To simplify the design in DCT-unconstrained case, we set $\widetilde{\boldsymbol{\mathcal{U}}}$ and $\widetilde{\boldsymbol{\mathcal{V}}}$ in Eq. (6) as $N\times N$ arbitrary unitary matrices, where $\widetilde{\boldsymbol{\mathcal{U}}}$ is designed such that it has structural one-degree regularity [10] to achieve good image coding. Table I compares of the CGs[dB] of the XBL-LTs in the DCT-constrained and unconstrained cases. In addition, Fig. 3 shows the frequency responses of the analysis and synthesis parts of the XBL-LTs for the same cases as in Table I. In Table I and Fig. 3, the DCT-unconstrained case had slightly better results than the DCT-constrained case. Table II shows the numbers of rounding operations of BL-LTs. It is clear that the XBL-LTs have fewer rounding operations than those of conventional BL-LTs.

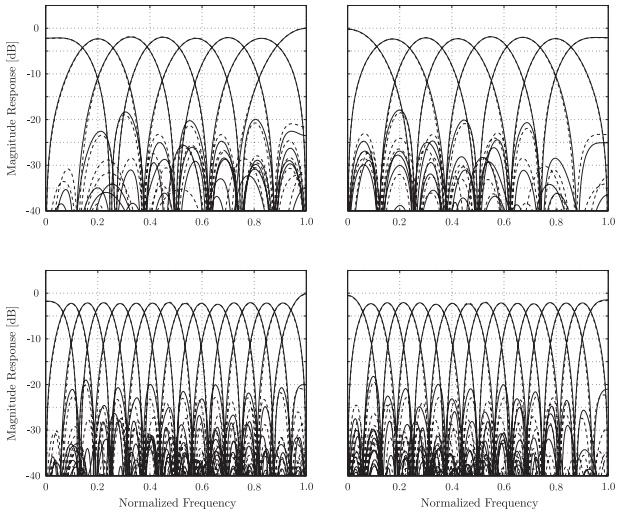

Fig. 3. Frequency responses of analysis and synthesis parts of XBL-LTs (dashed and solid lines indicate DCT-constrained and unconstrained cases, respectively): (top) 8×16 XBL-LT, (bottom) 16×32 XBL-LT.

B. Lossy-to-Lossless Image Coding

For convenience regarding the number of pages, lossy-to-lossless image coding was implemented in only the $M=8$ case. We used L-LTs in [7], [9], [11], [12] as the conventional L-LTs. The L-LT in [7] is the 4×8 L-LT for JPEG XR. The L-LT in [9] is the 8×16 TDLT with the pre-filtering part indicated by Cfg. 5 in Table V in [9] and the DCT part indicated by [15]. The L-LTs in [11], [12] are the DCT-constrained BL-LTs. After the images were transformed by the L-LTs and periodic extension at the boundaries, the transformed coefficients were rearranged from the subband mode to the multiresolution mode similar to the wavelet transform. They were encoded with a common wavelet-based zerotree

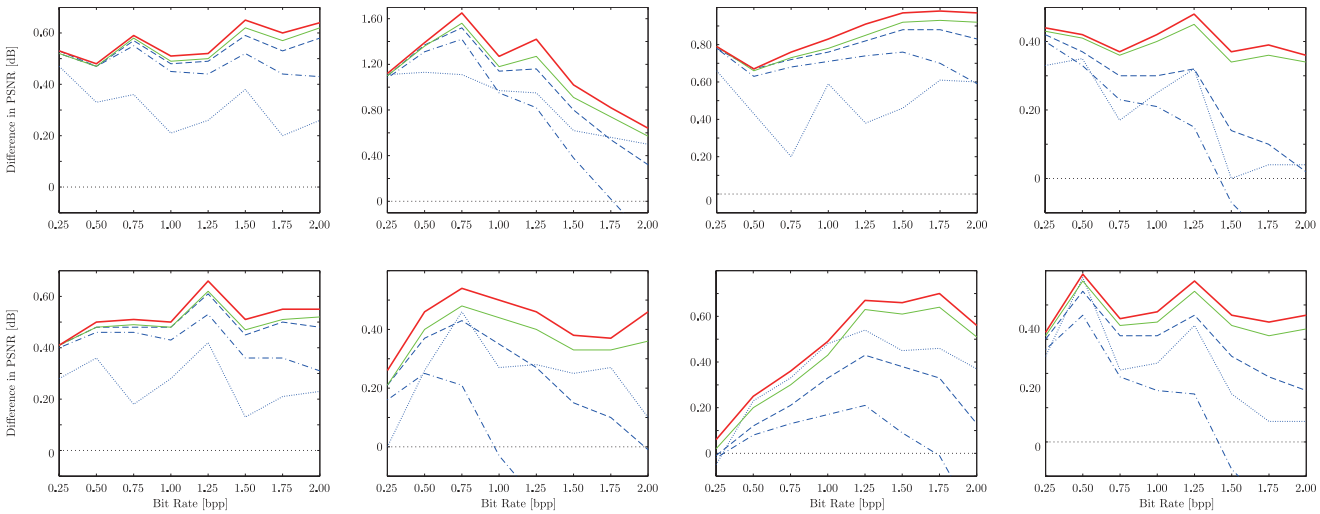

Fig. 4. Results of lossy image coding (blue dotted, blue chained, blue dashed, green solid, and red bold solid lines indicate 8×16 L-LT in [9], 8×16 BL-LT in [11], 8×16 BL-LT in [12], 8×16 DCT-constrained XBL-LT, and 8×16 DCT-unconstrained XBL-LT, respectively): (top) *Baboon*, *Barbara*, *Finger*, and *Goldhill*, (bottom) *Grass*, *Lena*, *Pepper*, and *Tank*.

TABLE III
RESULTS OF LOSSLESS IMAGE CODING (LBR [BPP], (α) AND (β) MEAN DCT-CONSTRAINED AND DCT-UNCONSTRAINED CASES, RESPECTIVELY.)

Test	L-LTs		BL-LTs		XBL-LTs	
Images	[7]	[9]	[11]	[12]	(α)	(β)
Baboon	6.23	6.26	6.21	6.21	6.21	**6.20**
Barbara	4.96	4.90	4.90	4.86	4.84	**4.83**
Boat	5.20	5.15	5.16	5.14	5.13	**5.12**
Elaine	5.27	5.24	5.26	**5.23**	**5.23**	**5.23**
Finger	5.89	5.92	5.84	**5.82**	**5.82**	**5.82**
Finger2	5.62	5.64	5.55	5.53	5.52	**5.51**
Goldhill	5.12	5.17	5.15	5.12	**5.11**	**5.11**
Grass	6.09	6.14	6.08	6.07	6.07	**6.06**
Lena	4.63	4.64	4.66	4.62	4.61	**4.60**
Pepper	5.00	4.93	4.96	4.93	4.92	**4.91**
Room	4.47	4.51	4.55	4.48	4.46	**4.44**
Sakura	5.94	6.03	5.95	5.93	5.92	**5.90**
Station	5.16	5.25	5.21	5.16	5.15	**5.14**
Tank	5.16	5.19	5.18	5.16	**5.15**	**5.15**

coder (SPIHT) [16]. The XBL-LTs were compared with the conventional L-LTs by using the lossless bit rate (LBR) and peak-to-noise ratio (PSNR) in lossy-to-lossless image coding:

$$\text{LBR [bpp]} = \frac{\text{Total number of bits [bit]}}{\text{Total number of pixels [pixel]}}$$

$$\text{PSNR [dB]} = 10 \log_{10} \left(\frac{255^2}{\text{MSE}} \right).$$

Table III and Fig. 4 show the results of lossless and lossy image coding. The vertical axes in Fig. 4 are the differences in PSNRs relative to the 4×8 L-LT in [7] for JPEG XR. It is clear that the XBL-LTs outperformed the conventional L-LTs in lossy-to-lossless image coding. In particular, although lifting-based transforms tended to degrade coding performance at high bit rates, the XBL-LTs preserved coding performance even at such high bit rates.

V. CONCLUSION

By extending an original LT and using block-lifting factorization, we developed an XBL-LT with fewer rounding operations. It is DCT-unconstrained and hence can be DCT-constrained as well; i.e., it can be considered to be a more general structure than other BL-LTs. Although we constrained the design by using unitary matrices in this paper, the DCT-unconstrained structures have the potential to achieve better coding.

ACKNOWLEDGMENT

This work was supported by JSPS Grant-in-Aid for Young Scientists (B), Grant Number 25820152.

REFERENCES

[1] H. S. Malvar, *Signal Processing with Lapped Transforms*, Norwood, MA: Artech House, 1992.
[2] K. R. Rao and P. Yip, *Discrete Cosine Transform Algorithms*, Academic Press, 1990.
[3] G. K. Wallace, "The JPEG still picture compression standard," *IEEE Trans. Consum. Electr.*, vol. 38, no. 1, pp. xviii–xxxiv, Feb. 1992.
[4] T. Wiegand, G. J. Sullivan, G. Bjøntegaard, and A. Luthra, "Overview of the H.264/AVC video coding standard," *IEEE Trans. Circuits Syst. Video Technol.*, vol. 13, no. 7, pp. 560–576, July 2003.
[5] G. J. Sullivan, J.-R. Ohm, W.-J. Han, and T. Wiegand, "Overview of the high efficiency video coding (HEVC) standard," *IEEE Trans. Circuits Syst. Video Technol.*, vol. 22, no. 12, pp. 1649–1668, Dec. 2012.
[6] W. Sweldens, "The lifting scheme: A custom-design construction of biorthogonal wavelets," *Appl. Comput. Harmon. Anal.*, vol. 3, no. 2, pp. 186–200, Apr. 1996.
[7] C. Tu, S. Srinivasan, G. J. Sullivan, S. Regunathan, and H. S. Malvar, "Low-complexity hierarchical lapped transform for lossy-to-lossless image coding in JPEG XR/HD Photo," in *Proc. of SPIE*, San Diego, CA, Aug. 2008, vol. 7073, pp. 1–12.
[8] F. Dufaux, G. J. Sullivan, and T. Ebrahimi, "The JPEG XR image coding standard," *IEEE Signal Process. Mag.*, vol. 26, no. 6, pp. 195–199, 204, Nov. 2009.
[9] T. D. Tran, J. Liang, and C. Tu, "Lapped transform via time-domain pre- and post-filtering," *IEEE Trans. Signal Process.*, vol. 6, no. 6, pp. 1557–1571, June 2003.
[10] T. Suzuki, M. Ikehara, and T. Q. Nguyen, "Generalized block-lifting factorization of M-channel biorthogonal filter banks for lossy-to-lossless image coding," *IEEE Trans. Image Process.*, vol. 21, no. 7, pp. 3220–3228, July 2012.
[11] T. Suzuki and M. Ikehara, "Integer fast lapped transforms based on direct-lifting of DCTs for lossy-to-lossless image coding," *EURASIP J. Image. Video Process.*, vol. 2013, no. 65, pp. 1–9, Dec. 2013.

[12] T. Suzuki and H. Kudo, "Integer fast lapped biorthogonal transform via applications of DCT matrices and dyadic-valued factors for lifting coefficient blocks," in *Proc. of ICIP'13*, Merboulne, Australia, Sep. 2013, pp. 800–804.
[13] T. Suzuki and M. Ikehara, "Integer DCT based on direct-lifting of DCT-IDCT for lossless-to-lossy image coding," *IEEE Trans. Image Process.*, vol. 19, no. 11, pp. 2958–2965, Nov. 2010.
[14] G. Strang and T. Nguyen, *Wavelets and Filter Banks*, Wellesley-Cambridge Press, 1996.
[15] S. Fukuma, K. Ohyama, M. Iwahashi, and N. Kambayashi, "Lossless 8-point fast discrete cosine transform using lossless Hadamard transform," Tech. Rep. of IEICE, DSP99-103, Oct. 1999.
[16] A. Said and W. A. Pearlman, "A new, fast, and efficient image codec based on set partitioning in hierarchical trees," *IEEE Trans. Circuits Syst. Video Technol.*, vol. 6, no. 3, pp. 243–250, June 1996.